Article

Time-Gated Imaging of Latent Fingerprints and Specific Visualization of Protein Secretions via Molecular Recognition

Jie Wang, Qinqin Ma, Haoyang Liu, Yingqian Wang, Haijing Shen, Xiaoxia Hu, Chao Ma, Quan Yuan, and Weihong Tan

Anal. Chem., **Just Accepted Manuscript** • DOI: 10.1021/acs.analchem.7b03003 • Publication Date (Web): 07 Nov 2017

Time-Gated Imaging of Latent Fingerprints and Specific Visualization of Protein Secretions *via* Molecular Recognition

Jie Wang,[†] Qinqin Ma,[†] Haoyang Liu,[†] Yingqian Wang,[†] Haijing Shen,[†] Xiaoxia Hu,[†] Chao Ma,[#] Quan Yuan*,[†] Weihong Tan[‡]

[†]Key Laboratory of Analytical Chemistry for Biology and Medicine (Ministry of Education), College of Chemistry and Molecular Sciences, Wuhan University, Wuhan 430072, China

[‡]Molecular Science and Biomedicine Laboratory, State Key Laboratory of Chemo/Bio-sensing and Chemometrics, College of Chemistry and Chemical Engineering, College of Biology, Collaborative Innovation Center for Chemistry and Molecular Medicine, Hunan University, Changsha 410082, China

[#]Center for High Resolution Electron Microscopy, College of Materials Science and Engineering, Hunan University, Changsha 410082, China

*Corresponding Author:

Prof. Quan Yuan

Tel/Fax: +86-27-68756362

E-mail: yuanquan@whu.edu.cn

ABSTRACT: Persistent nanophosphors can remain luminescent after excitation ceases, thus they offer a promising way to avoid background fluorescence interference in bioimaging. In this work, Zn_2GeO_4:Ga,Mn (ZGO:Ga,Mn) persistent luminescence nanoparticles were developed and they were employed for time-gated imaging of latent fingerprints (LFP). The nanoparticles were functionalized with carboxyl group and utilized to label LFP through reacting with amino group in LFP. Results proved the potent ability of ZGO:Ga,Mn in eliminating background fluorescence to afford highly sensitive LFP imaging. Moreover, LFP aged for 60 days were successfully detected due to the presence of highly stable amino acids. After functionalized with concanavalin A, the nanoparticles achieved visualization of glycoproteins in LFP. This strategy provides great versatility in LFP imaging and good potential in uncovering the chemical information within LFP, making it valuable in forensic investigations and medical diagnostics.

Fingerprints hold a wealth of information, ranging from the friction ridge patterns to the metabolism of the donors.[1-3] Thus fingerprints detection has gained tremendous interest in areas such as forensic investigation, medical diagnostics and health assessment.[4-7] Latent fingerprints (LFP) are the most commonly encountered forms of fingerprints and are also the most problematic because they are present but invisible.[8,9] Detection of LFP has attracted considerable attention[10-16] and lots of methods have been developed.[17-19] Among all of the techniques, photoluminescence detection of LFP has brought about a new level of sensitivity and selectivity.[20-23] Despite the many positive attributes, photoluminescence still faces great challenges, most notably background fluorescence.[2,20] For fingerprints on substrates with background fluorescence, the obtained images are usually seriously blurred or even completely buried,[2] which seriously decreases the sensitivity and resolution. To negate background fluorescence, phosphors with emissions at different wavelengths than the background have been developed.[24-27] In spite of such advances, phosphors that can completely avoid background fluorescence is still in urgent need for LFP detection.

Persistent phosphors can remain luminescent for several seconds to few days after the cease of excitation.[28-34] In the past years, persistent phosphors have been widely employed in bioimaging[35-39] and superior signal-to-noise ratio was achieved in small animals imaging due to the avoiding of tissue autofluorescence.[40-44] In LFP imaging, persistent phosphor can also efficiently eliminate background fluorescence interference, since the fingerprint images can be collected after the short-lived background fluorescence has completely decayed. Accordingly, persistent nanophosphors are ideal for LFP imaging.

Herein, Zn_2GeO_4:Ga,Mn (ZGO:Ga,Mn) persistent luminescence nanoparticles are directly synthesized with hydrothermal method. The strategy for background-free covalent labelling of LFP with the ZGO:Ga,Mn nanoparticles is illustrated in Scheme 1. The nanoparticles are functionalized with carboxyl groups (ZGO:Ga,Mn-COOH) and further treated with EDC/NHS to form active esters on their surface. The nanoparticles are further applied to a LFP and the active esters can react with intrinsic amino groups in the ridges to form covalent bonds, resulting in strong labelling of the LFP. Under excitation, the substrate displays strong background fluorescence and the fingerprint image is seriously blurred. However, after excitation ceases, the background fluorescence decays rapidly but the nanoparticles remain luminescent, leading to appearance of a clear fingerprint image. Moreover, due to the high stability of amino acids, LFP aged for 60 days

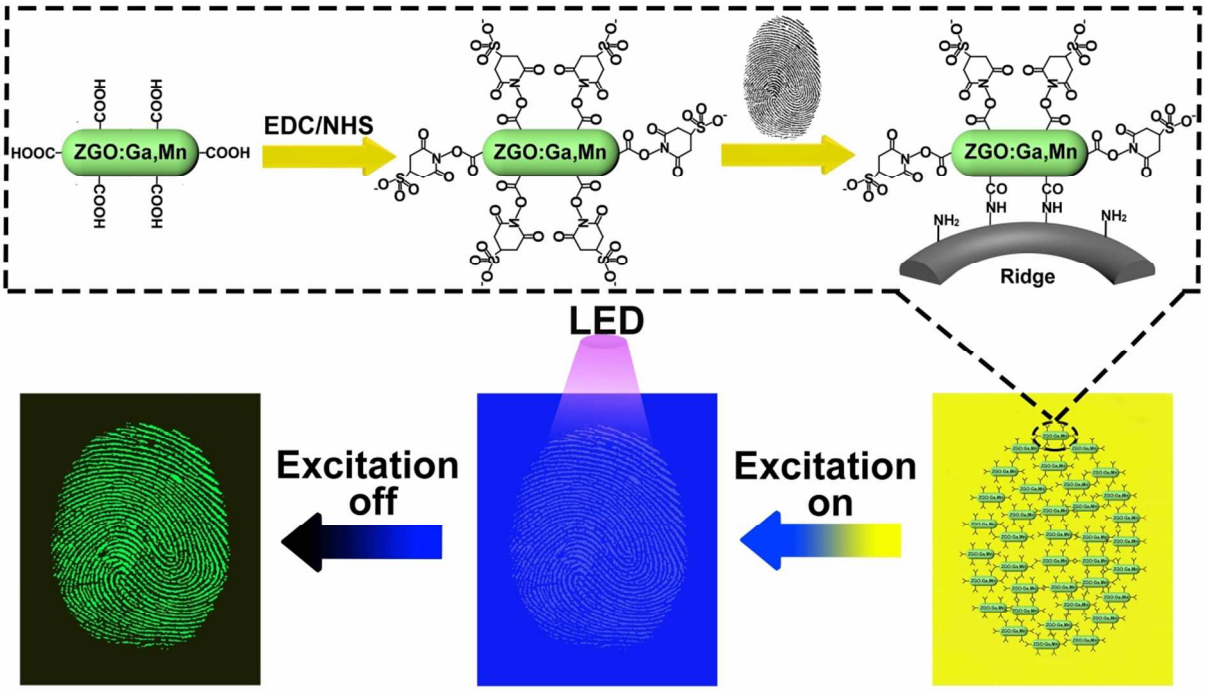

Scheme 1. Schematic illustration of time-gated imaging of fingerprints with ZGO:Ga,Mn-COOH nanoparticles.

can be easily detected. Additionally, after functionalization with concanavalin A (ConA), the ZGO:Ga,Mn nanoparticles were further successfully applied in imaging of glycoproteins in LFP. The outstanding performances of ZGO:Ga,Mn in LFP imaging may further contribute to areas such as forensic investigation and medical diagnostics.

EXPERIMENTAL SECTION

Synthesis of Zn_2GeO_4:1.0%Ga,0.5%Mn (ZGO:Ga,Mn) nanoparticles. The ZGO:Ga,Mn nanoparticles were synthesized with a hydrothermal method.[29,34,45] Briefly, 1.96 mmol $Zn(NO_3)_2$, 0.01 mmol $Ga(NO_3)_3$, 0.005mmol $Mn(NO_3)_2$, 300 μL HNO_3 were dissolved in 11 mL deionized water. Then, 0.96 mmol Na_2GeO_3 was dropwise added in the solution. After that, ammonium hydroxide (28%, wt) was immediately added into the above solution to adjust the pH value to around 9.5 under vigorous stirring. Then the mixture was left stirring for 1 h at room temperature (20-30 °C). After that, the solution was transferred into a Teflon-lined autoclave and reacted at 220 °C for 6 h. The as prepared ZGO:Ga,Mn nanoparticles were collected by centrifugation and washed with deionized water for three times.

Measuring the decay images of ZGO:Ga,Mn nanoparticles. The ZGO:Ga,Mn nanoparticles (0.1 g) were put into a well of a 48-well-plate. Then the nanoparticles were illuminated with a portable ZF-5 UV lamp for 3 min. After that, the plate was immediately put into the Bruker *In Vivo*-Xtreme Imaging System to record the decay images at different time.

Preparation of ZGO:Ga,Mn-COOH nanoparticles. The directly synthesized ZGO:Ga,Mn nanoparticles were firstly functionalized with amino groups (ZGO:Ga,Mn-NH_2). Then, the carboxyl groups were grafted to the surface of ZGO:Ga,Mn nanoparticles via reacting with succinic anhydride. The preparation of ZGO:Ga,Mn-NH_2 nanoparticles was performed as follows. Briefly, 50 mg of ZGO:Ga,Mn nanoparticles was dispersed in 20 mL of N,N-dimethylformamide (DMF) by sonication. Then 200 μL of APTES was dropwise added into the solution under vigorous stirring. The reaction mixture was kept at 80 °C for 12 h under vigorous stirring. The obtained ZGO:Ga,Mn-NH_2 nanoparticles were washed with DMF for three times to remove the unreacted APTES. Then, the as-prepared ZGO:Ga,Mn-NH_2 nanoparticles were dispersed in 30 mL of DMF. After that, 10 mL of succinic anhydride solution (5 mg/mL in DMF) and 10 mL of DMAP solution (0.5 mg/mL in DMF) were added into the nanoparticles solution and the mixture was stirred for 12 h at room temperature (20-30 °C). The resultant ZGO:Ga,Mn-COOH nanoparticles were washed three times with ethanol/water (v/v, 1:1) and then dispersed in 25 mL of deionized water for further usage.

Latent fingerprints collection. Fingerprint samples were collected from five healthy donors (three females and two males: female 1, 23 years old; female 2, 24 years old; female 3, 25 years old; male 1, 23 years old; male 2, 26 years old).[46] A variety of substrates were tested (poker card; soft drink can, aluminum foil, knife, desk, plastic Petri dish, green leaf, and glass microscope slide). For fingerprints collection on glass microscope slides, a pretreatment procedure was applied to the slides. Typically, the glass slides were immersed in the APTES solution (1%, v/v in DMF) for one day at room temperature (20-30 °C). Then the slides were further immersed in the glutaraldehyde aqueous solution (25%) for another day to block the hydroxyl groups on the glass slides. All of the donors did not wash their hands within 1 h before the collection, and they were asked to press their fingers on the chosen substrates to deposit the latent fingerprints. The obtained fingerprints were aged for at least 12 h at room temperature (20-30 °C) in dark before the development. In the detection of aged fingerprints, donors were asked to press their fingers on aluminum foil, and the deposited fingerprints were further aged for different time length (12 h to 60 days) at room temperature (20-30 °C) in dark.

Activation of the ZGO:Ga,Mn-COOH nanoparticles with EDC/NHS. Typically, 10 mL of the ZGO:Ga,Mn-COOH

nanoparticles solution was centrifuged and the supernatant was removed. Then, EDC (50 mg) and NHS (25 mg) were dissolved in 2 mL and 3 mL PB buffer (10 mM, pH=6.8), respectively. The above ZGO:Ga,Mn-COOH nanoparticles were dispersed in the EDC solution by sonication, and the NHS solution was also instantly added into the nanoparticles dispersion. The resultant solution was allowed to react at 37 °C for 30 min under gentle shaking (200 r/min). After that, the activated ZGO:Ga,Mn-COOH nanoparticles were washed with PB buffer (10 mM, pH=7.2) and further re-dispersed in 10 mL of PB buffer (10 mM, pH=7.2).

Fingerprints imaging with the activated ZGO:Ga,Mn-COOH nanoparticles. Briefly, 200 μl of the activated ZGO:Ga,Mn-COOH nanoparticles solution (1 mg/mL in PB buffer, pH=7.2) was added on the fingerprints and the fingerprints were left at room temperature (20-30 °C) for 30 min. After that, the solution was removed with a micropipette and the fingerprints were carefully rinsed with PB buffer (10 mM, pH=7.2) to remove the unreacted nanoparticles. The as-treated fingerprints were irradiated with a portable ZF-5 UV lamp and the images were captured by a digital single-lens reflex camera. For fingerprints imaging on substrates with background fluorescence, a video was recorded with the digital single-lens reflex camera when the UV lamp was tuned off. Then the video was further played with the potplayer (Daum, 1.6.60136.0) to pick out the screens of fingerprint images that were not interfered by the background fluorescence from substrates.

Confocal measurement. Fingerprints were labeled with a near-infrared dye DiD before treatment with the nanoparticles solution. Typically, 10 μL of DiD solution (5 nM) was applied to the fingertips of donors and the solution was further spread on the fingertips with a micropipette. After drying for about 10 min, donors were asked to blot their fingers on the pretreated glass microscope slides. The as-labeled fingerprints were aged for 12 h and further treated with the activated ZGO:Ga,Mn-COOH nanoparticles. The as-treated fingerprints were further captured by the confocal laser scanning microscope.

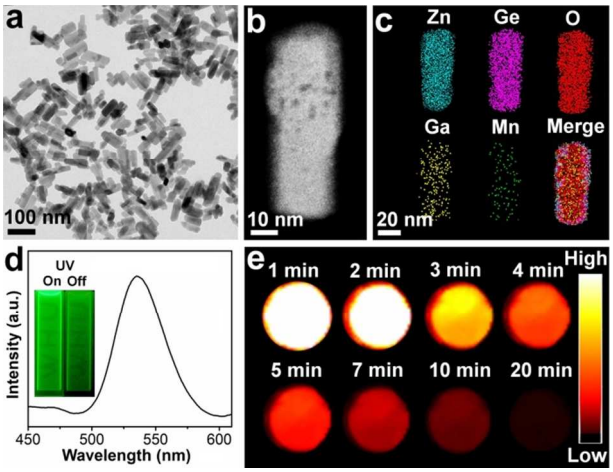

Figure 1. (a) TEM image of ZGO:Ga,Mn-COOH nanoparticles. (b) HAADF-STEM and (c) corresponding elemental mapping images of a single ZGO:Ga,Mn-COOH nanoparticle. (d) Photoluminescence spectrum of the ZGO:Ga,Mn-COOH nanoparticles. Inset: nanoparticles dispersion under excitation and after excitation ceases. (e) Images of the luminescence decay in ZGO:Ga,Mn-COOH nanoparticles.

Preparation of ZGO:Ga,Mn-ConA nanoparticles. Typically, 5 mg of ConA was dissolved in 10 mL of the activated ZGO:Ga,Mn-COOH nanoparticles solution (1 mg/mL), and the solution was allowed to react at 37 °C for 6 h under gentle shaking (180 r/min). The resultant ZGO:Ga,Mn-ConA nanoparticles were washed with PB buffer (10 mM, pH=7.2) for 2 times and further re-dispersed in 10 mL of PB buffer (10 mM, pH=7.2).

Fingerprints imaging with ZGO:Ga,Mn-ConA nanoparticles. Briefly, the fingerprints were incubated with the ZGO:Ga,Mn-ConA nanoparticles solution (1 mg/mL) for about 40 min at room temperature (20-30 °C). Then the solution was removed and the fingerprints were carefully rinsed with PB buffer. The images of the treated fingerprints were captured with a digital single-lens reflex camera under the excitation of a portable ZF-5 UV lamp. In the control group, fingerprints were treated with ZGO:Ga,Mn-COOH nanoparticles without ConA functionalization, and the nanoparticles were not activated with EDC and NHS.

RESULTS AND DISCUSSION

Characterization of the ZGO:Ga,Mn-COOH nanoparticles. Transmission electron microscopy (TEM) image (Figure 1a) shows that the ZGO:Ga,Mn-COOH nanoparticles are well-dispersed with average length of about 60 nm. Elemental mapping images (Figure 1b and 1c) indicate the homogeneous distribution of doped Ga^{3+} and Mn^{2+} ions in the nanoparticles. The luminescence band of ZGO:Ga,Mn-COOH nanoparticles is peaking at about 540 nm (Figure 1d). The inset in Figure 1d shows that the nanoparticles dispersion displays bright green luminescence after the ceases of excitation, suggesting the strong persistent luminescence in the developed nanoparticles. The visualized images of the luminescence decay in ZGO:Ga,Mn-COOH nanoparticles are shown in Figure 1e. It is observed that the nanoparticles remain luminescent even after 20 min of decay, which ensures adequate time for the capture of fingerprint images after excitation is switched off.

Background-free fingerprints imaging based on the ZGO:Ga,Mn-COOH nanoparticles. Daily encountered substrates were employed to test the ability of ZGO:Ga,Mn-COOH nanoparticles in eliminating background fluorescence. A fingerprint was deposited on a poker card and further

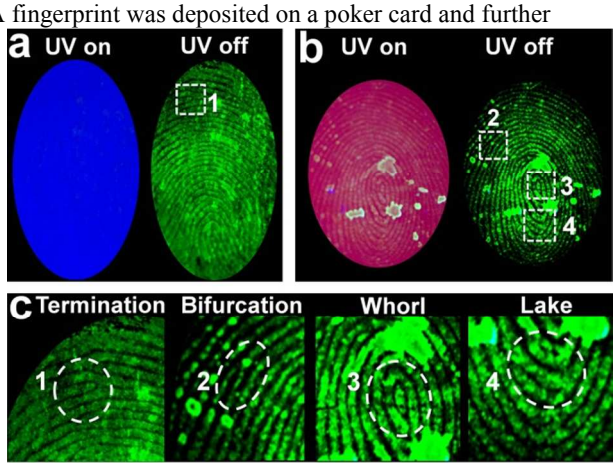

Figure 2. (a) Photograph of a treated fingerprint on a poker card under excitation and after excitation ceases. (b) Photograph of a treated fingerprint on a soft drink can under excitation and after excitation ceases. (c) Specific details of the fingerprints.

labelled with the ZGO:Ga,Mn-COOH nanoparticles (Figure S7). Under excitation (Figure 2a, left image), the poker card displays strong blue fluorescence and the luminescence from fingerprint is completely buried. Such phenomenon is usually encountered in LFP imaging on problematic surfaces. However, after the cease of excitation (Figure 2a, right image), the blue background fluorescence disappears completely and a legible fingerprint image appears. Moreover, the obtained image displays bright, well-resolved ridge flow and pattern structure, which forms the basis of personal identification. LFP imaging on another substrate with background fluorescence was also investigated. A latent fingerprint was deposited on the logo of a soft drink can. As shown in Figure 2b, the logo displays strong red back ground fluorescence under excitation, which significantly decreases the resolution of the fingerprint (Figure 2b, left image). After the excitation was switched off, a bright fingerprint image with clear ridge pattern was obtained (Figure 2b, right image). It is worth noting that the high quality of the obtained fingerprint images enables visualization of specific details. As shown in Figure 2c, fingerprint details such as termination, bifurcation, whorl and lake can be clearly visualized at higher magnification, which makes the fingerprint unique and can thus provide valuable information for personal identification. Additionally, the capability of this time-gated imaging method in reducing background fluorescence was compared with the optical filtering method[20] (Figure S8). Results show that optical filtering becomes inefficient when the emission wavelengths of the background chromophores and the imaging probe are overlapped. On the contrary, the time-gated imaging method based on ZGO:Ga,Mn-COOH persistent luminescence nanoparticles can efficiently eliminate background fluorescence interference regardless of the emission wavelength. The above results thus clearly demonstrated that the time-gated imaging strategy possesses great versatility in eliminate background fluorescence interference, making it valuable in LFP imaging.

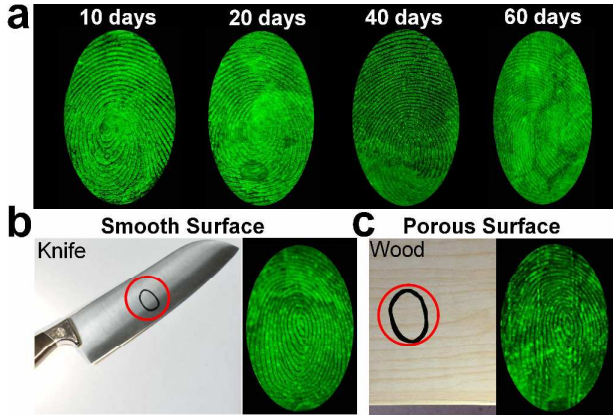

Figure 3. (a) Luminescent images of fingerprints aged for time lengths. (b) Images of fingerprints on smooth (a knife) and (c) porous (a desk) surfaces.

Aged fingerprints and fingerprints on different surfaces. Fingerprints encountered in real situations are often aged rather than freshly deposited.[47] Aging of fingerprints presents a significant challenge for LFP detection because the loss of water, chloride ions, and other substances[47] usually makes detection techniques ineffective.[48] Previous studies reported that amino acids in fingerprints are very stable and can even last for decades.[47] Therefore, this covalent labelling strategy holds good promise for the detection of aged fingerprints. The ZGO:Ga,Mn-COOH nanoparticles were further employed for aged fingerprints imaging. As shown in Figure 3a and Figure S9, all of the aged fingerprints can be easily detected, and one can clearly see the finely-resolved ridge details. It is worth noting that even 60-day old fingerprint is clearly observed without noticeable loss of resolution. The ZGO:Ga,Mn-COOH nanoparticles were further employed for LFP imaging on both smooth and porous surfaces. The image of a LFP on a knife shows clear discrimination between ridges and grooves (Figure 3b). LFP imaging on porous wood was also performed (Figure 3c). The treated fingerprint displays strong luminescence without any loss of the friction ridge details. The above results clearly demonstrate that the ZGO:Ga,Mn nanoparticles can not only be applied to the detection of aged fingerprints, but also can be utilized in LFP imaging on different substrates, suggesting its great versatility in meeting the various demands in LFP detection.

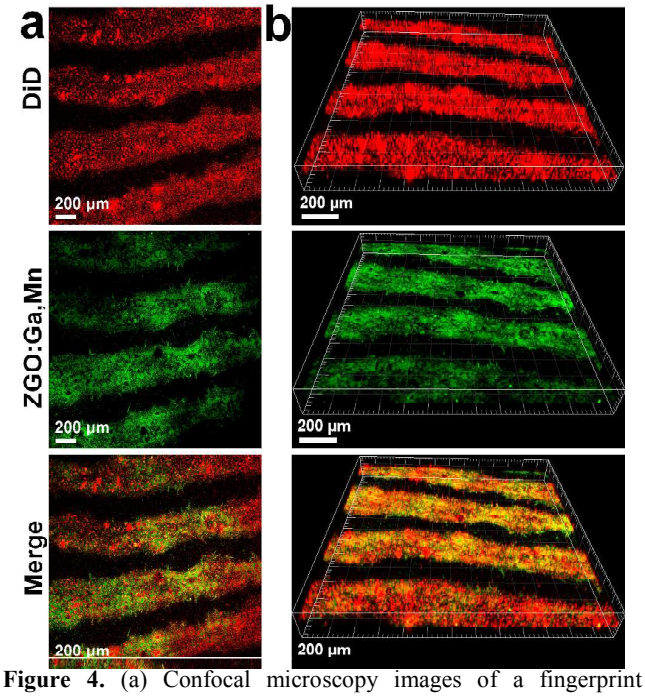

Figure 4. (a) Confocal microscopy images of a fingerprint labelled with a commercial dye (DiD, red channel). The fingerprint was further treated with ZGO:Ga,Mn-COOH nanoparticles (green channel). (b) The corresponding 3D view of the fingerprint ridges.

The binding of ZGO:Ga,Mn-COOH nanoparticles to fingerprint ridges. The binding of ZGO:Ga,Mn-COOH nanoparticles to the fingerprint ridges was confirmed by laser scanning confocal microscopy. The fingers of donors were stained with the solution of a commercial dye DiD. After the donors pressing their fingers on glass slides, the DiD labelled fingerprints were obtained. The fingerprints were further treated with the activated ZGO:Ga,Mn-COOH nanoparticles. As shown in Figure 4a, the signal from the DiD clearly indicates the fingerprint ridges (red channel). After treated with the activated ZGO:Ga,Mn-COOH dispersion, signal from the nanoparticles appears with the same ridges pattern (green channel). Overlay of the two channels shows that the green luminescence is exactly on the ridges of fingerprints. The binding of the ZGO:Ga,Mn-COOH nanoparticles to fingerprint ridges is further demonstrated by the 3D view of the ridges (Figure 4b).

Comparing the fingerprint detection performance of ZGO:Ga,Mn-COOH nanoparticles with a commercial black fingerprint powder. To further investigate the future practical applications of the ZGO:Ga,Mn-COOH nanoparticles, the ZGO:Ga,Mn-COOH was compared with a commercial black fingerprint powder for both freshly deposited and aged fingerprints detection. As shown in Figure 5a and 5b, the freshly deposited fingerprints treated with the ZGO:Ga,Mn-COOH nanoparticles and the black fingerprint powder all display finely-resolved ridge details. The luminescent fingerprint image in Figure 5a was further converted into gray scale image (Figure S10a) and the variation of gray value over the fingerprints indicated by the solid yellow line (in Figure 5a and 5b) was shown in Figure 5c. The gray value varies significantly across the fingerprints treated with the ZGO:Ga,Mn-COOH nanoparticles, and the ridges and furrows of the fingerprint can be clearly recognized. However, for fingerprints treated with the black fingerprint powder, insignificant variation of the gray value is observed, making it difficult to discriminate the ridges and furrows. Figure 5d shows that the aged fingerprint developed with ZGO:Ga,Mn-COOH nanoparticles still displays clear rigid patterns. In contrast, serious loss of friction ridge details is observed when the aged fingerprint is treated with the black fingerprint powder (Figure 5e). The variation of gray value over the fingerprints (Figure 5f) further suggests that the ZGO:Ga,Mn-COOH nanoparticles displays high contrast ratio even in aged fingerprints detection. The above results thus clearly reveal that the ZGO:Ga,Mn-COOH nanoparticles display better performance in fingerprints detection than the commercial black fingerprint powder.

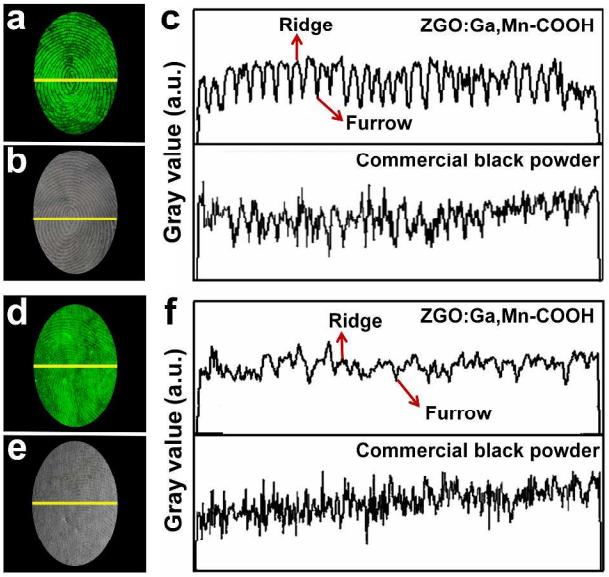

Figure 5. (a) Images of freshly deposited fingerprints treated with the ZGO:Ga,Mn-COOH nanoparticles and (b) a commercial black fingerprint powder. (c) Variation of the gray value over the fingerprints indicated by the solid yellow line shown in (a) and (b). (d) Images of 20 days old fingerprints treated with the ZGO:Ga,Mn-COOH nanoparticles and (e) a commercial black fingerprint powder. (f) Variation of the gray value over the fingerprints indicated by the solid yellow line shown in (d) and (e). The fingerprints were deposited on aluminum foil. Conversion of the color images (a, d) into gray scale images and quantification of the gray value variations were all performed with the Quantity One® Software (Bio-Rad, Version 4.6.9).

Detection of glycoproteins in fingerprint with ZGO:Ga,Mn-ConA nanoparticles. Fingerprints contain varying kinds of metabolites,[47] including glycoproteins.[49] Previous studies reported that glycoproteins play crucial roles in molecular processes such as immunesurveillance,[50] and they are also representative biomarkers for cancer.[51] The ZGO:Ga,Mn-COOH nanoparticles were further functionalized with ConA,[52] a lectin with strong binding affinity towards glycoproteins, for the detection of glycoproteins in fingerprints (Figure 6a). The luminescent images of fingerprints treated with the ConA modified ZGO:Ga,Mn nanoparticles (ZGO:Ga,Mn-ConA) are presented in Figure 6b and Figure S14. Well-resolved ridge patterns with good separation between furrows and ridges are clearly observed. The above images can offer chemical information about the metabolism of donors, providing valuable information for medical diagnostics. In contrast, fingerprints treated with the ZGO:Ga,Mn-COOH nanoparticles do not show ridge patterns (Figure 6c), indicating the specific recognition capability of the ZGO:Ga,Mn-ConA nanoparticles. The above results thus suggest the good potential of the proposed method in health assessment.

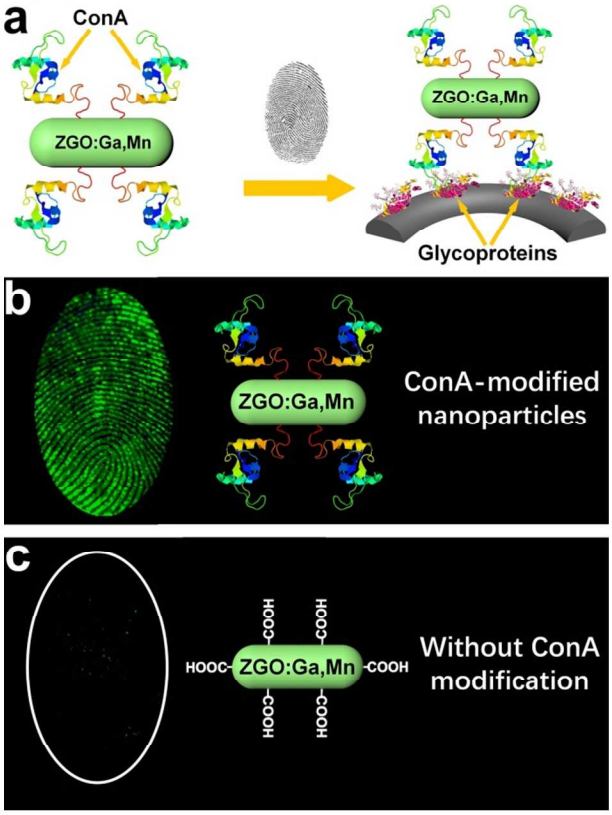

Figure 6. (a) Detection of glycoproteins in LFP. (b) Images of LFP treated with ZGO:Ga,Mn-ConA and (c) the unmodified ZGO:Ga,Mn-COOH nanoparticles.

CONCLUSIONS

In this work, we have highlighted the special advantages of ZGO:Ga,Mn nanoparticles in eliminating the interference from background fluorescence in LFP imaging. Fingerprints on daily encountered substrates with background fluorescence can be readily visualized using ZGO:Ga,Mn-COOH nanoparticles, and the obtained LFP images display well-resolved specific details. The ZGO:Ga,Mn-COOH nanoparticles can further be applied in the detection of

fingerprints aged for long times. Besides, LFP on different kinds of substrates were also easily detected. Furthermore, chemical secretions with biomedical or diagnostic values can also be readily visualized with functionalized ZGO:Ga,Mn nanoparticles. To conclude, ZGO:Ga,Mn nanoparticles show great versatility in avoiding background interference, and they also show promise in revealing the many different types of information in fingerprints. Thus ZGO:Ga,Mn nanoparticles will be valuable in wide-ranging applications such as forensic investigations, medical diagnostics and health assessment.

ASSOCIATED CONTENT

Supporting Information

TEM images and XRD pattern of the ZGO:Ga,Mn nanoparticles, TEM images of the ZGO:Ga,Mn-NH_2 nanoparticles, ZGO:Ga,Mn-COOH nanoparticles and ZGO:Ga,Mn-ConA nanoparticles, decay spectrum of the ZGO:Ga,Mn-COOH nanoparticles, photographs of the poker card and soft drink can substrates, luminescent images of fingerprints obtained with optical filtering and time-gated imaging, luminescent images of fingerprints aged for time lengths and fingerprints on different substrates, gray scale images of a freshly deposited and a 20 days old fingerprints developed with the ZGO:Ga,Mn-COOH nanoparticles, zeta potentials, luminescent images of fingerprints from different donors. The Supporting Information is available free of charge on the ACS Publications website.

AUTHOR INFORMATION

Corresponding Author

*yuanquan@whu.edu.cn

Author Contributions

All authors have given approval to the final version of the manuscript.

Notes

The authors declare no competing financial interest.

ACKNOWLEDGMENT

This work was supported by the National Natural Science Foundation of China (21422105, 21675120) and Ten Thousand Talents Program for Young Talents. We greatly thank Prof. Haibo Zeng at Nanjing University of Science and Technology for critical reading of the manuscript.

REFERENCES

(1) Ifa, D. R.; Manicke, N. E.; Dill, A. L.; Cooks, R. G. *Science* **2008**, *321*, 805.
(2) Wang, J.; Wei, T.; Li, X.; Zhang, B.; Wang, J.; Huang, C.; Yuan, Q. *Angew. Chem., Int. Ed.* **2014**, *53*, 1616-1620.
(3) Leggett, R.; Lee-Smith, E. E.; Jickells, S. M.; Russell, D. A. *Angew. Chem., Int. Ed.* **2007**, *46*, 4100-4103.
(4) Song, W.; Mao, Z.; Liu, X.; Lu, Y.; Li, Z.; Zhao, B.; Lu, L. *Nanoscale* **2012**, *4*, 2333-2338.
(5) Peng, T.; Qin, W.; Wang, K.; Shi, J.; Fan, C.; Li, D. *Anal. Chem.* **2015**, *87*, 9403-9407.
(6) Wood, M.; Maynard, P.; Spindler, X.; Roux, C.; Lennard, C. *Aust. J. Forensic Sci.* **2013**, *45*, 211-226.
(7) Brunelle, E.; Huynh, C.; Le, A.-M.; Halámková, L.; Agudelo, J.; Halámek, J. *Anal. Chem.* **2016**, *88*, 2413-2420.
(8) Wu, P.; Xu, C.; Hou, X.; Xu, J. J.; Chen, H. Y. *Chem. Sci.* **2015**, *6,* 4445-4450.
(9) Jaber, N.; Lesniewski, A.; Gabizon, H.; Shenawi, S.; Mandler, D.; Almog, J. *Angew. Chem., Int. Ed.* **2012**, *51*, 12224-12227.
(10) Li, K.; Qin, W.; Li, F.; Zhao, X.; Jiang, B.; Wang, K.; Deng, S.; Fan, C.; Li, D. *Angew. Chem., Int. Ed.* **2013**, *52*, 11542-11545.
(11) Song, K.; Huang, P.; Yi, C.; Ning, B.; Hu, S.; Nie, L.; Chen, X.; Nie, Z. *ACS Nano* **2015**, *9*, 12344-12348.
(12) Tang, X.; Huang, L.; Zhang, W.; Zhong, H. *Anal. Chem.* **2015**, *87*, 2693-2701.
(13) Hazarika, P.; Russell, D. A. *Angew. Chem., Int. Ed.* **2012**, *51*, 3524-3531.
(14) Xu, L.; Li, Y.; Wu, S.; Liu, X.; Su, B. *Angew. Chem., Int. Ed.* **2012**, *51*, 8068-8072.
(15) Hansen, D. B.; Joullié, M. M. *Chem. Soc. Rev.* **2005**, *34*, 408-417.
(16) He, Y.; Xu, L.; Zhu, Y.; Wei, Q.; Zhang, M.; Su, B. *Angew. Chem., Int. Ed.* **2014,** *53*, 12609-12612.
(17) Ramotowski, R. S.; Gaensslen, R. E. *Advances in Fingerprint Technology*, 2nd ed.; CRC press: Boca Raton, FL, 2001.
(18) Ramotowski, R. S. *Lee and Gaensslen's Advances in Fingerprint Technology*, 3rd ed.; CRC press: Boca Raton, FL, 2012.
(19) Margot, P.; Lennard, C. *Fingerprint Detection Techniques*, Université de Lausanne Institut de police scientifique et de criminologie, Switzerland, 1994.
(20) Menzel, E. R. *Sci. World J.* **2001**, *1*, 498-509.
(21) Chen, X.; Xu, W.; Zhang, L.; Bai, X.; Cui, S.; Zhou, D.; Yin, Z.; Song, H.; Kim, D. H. *Adv. Funct. Mater.* **2015**, *25*, 5462-5471.
(22) Xu, L. R.; Li, Y.; Li, S. H.; Hu, R. R.; Qin, A. J.; Tang, B. Z.; Su, B. *Analyst* **2014**, *139*, 2332-2335.
(23) Li, Y.; Xu, L. R.; Su, B. *Chem. Commun.* **2012**, *48*, 4109-4111.
(24) Jelly, R.; Lewis, S. W.; Lennard C.; Lim, K. F. *Chem. Commun.* **2008**, 3513-3515.
(25) Maynard, P.; Jenkins, J.; Edey, C.; Payne, G.; Lennard, C.; McDonagh A.; Roux, C. *Aust. J. Forensic Sci.* **2009**, *41*, 43-62.
(26) Chadwick, S.; Maynard, P.; Kirkbride, P.; Lennard, C.; McDonagh, A.; Spindler X.; Roux, C. *Forensic Sci. Int.* **2012**, *219*, 208-214.
(27) King, R. S. P.; Hallett P. M.; Foster, D. *Forensic Sci. Int.* **2015**, *249*, e21-e26.
(28) Li, Y.; Gecevicius, M.; Qiu, J. *Chem. Soc. Rev.* **2016**, *45*, 2090-2136.
(29) Li, Z.; Zhang, Y.; Wu, X.; Huang, L.; Li, D.; Fan, W.; Han, G. *J. Am. Chem. Soc.* **2015**, *137*, 5304-5307.
(30) Wu, B. Y.; Wang, H. F.; Chen, J. T.; Yan, X. P. *J. Am. Chem. Soc.* **2010**, *133*, 686-688.
(31) Kong, J.; Zheng, W.; Liu, Y.; Li, R.; Ma, E.; Zhu, H.; Chen, X. *Nanoscale* **2015**, *7*, 11048-11054.
(32) Pan, Z.; Lu, Y. Y.; Liu, F. *Nat. Mater.* **2012**, *11*, 58-63.
(33) Wang, J.; Ma, Q. Q.; Wang, Y. Q.; Shen, H. J.; Yuan, Q. *Nanoscale* **2017**, *9*, 6204-6218.
(34) Wang, J.; Ma, Q. Q.; Zheng, W.; Liu, H. Y.; Yin, C. Q.; Wang, F. B.; Chen, X. Y.; Yuan, Q.; Tan, W. H. *ACS Nano* **2017**, *11*, 8185-8191.
(35) Li, N.; Li, Y. H.; Han, Y. Y.; Pan, W.; Zhang, T. T.; Tang, B. *Anal. Chem.* **2014**, *86*, 3924-3930.
(36) Abdukayum, A.; Chen, J. T.; Zhao, Q.; Yan, X. P. *J. Am. Chem. Soc.* **2013**, *135*, 14125-14133.
(37) Shi, J.; Sun, X.; Li, J.; Man, H.; Shen, J.; Yu, Y.; Zhang, H. *Biomaterials* **2015**, *37*, 260-270.
(38) de Chermont, Q. l. M.; Chanéac, C.; Seguin, J.; Pellé, F.; Maîtrejean, S.; Jolivet, J. P.; Gourier, D.; Bessodes, M.; Scherman, D. *Proc. Natl. Acad. Sci. U. S. A.* **2007**, *104*, 9266-9271.
(39) Abdukayum, A.; Yang, C. X.; Zhao, Q.; Chen, J. T.; Dong, L. X.; Yan, X. P. *Anal. Chem.* **2014**, *86*, 4096-4101.
(40) Li, N.; Diao, W.; Han, Y.; Pan, W.; Zhang, T.; Tang, B. *Chem.-Eur. J.* **2014**, *20*, 16488-16491.
(41) Li, Y. J.; Yan, X. P. *Nanoscale* **2016**, *32*, 14965-14970.
(42) Maldiney, T.; Bessière, A.; Seguin, J.; Teston, E.; Sharma, S. K.; Viana, B.; Bos, A. J.; Dorenbos, P.; Bessodes, M.; Gourier, D. *Nat. Mater.* **2014**, *13*, 418-426.
(43) Wu, S. Q.; Chi, C. W.; Yang, C. X.; Yan, X. P. *Anal. Chem.* **2016**, *88*, 4114-4121.
(44) Shi, J.; Sun, X.; Zhu, J.; Li, J.; Zhang, H. *Nanoscale* **2016**, *8*, 9798-9804.
(45) Wang, J.; Ma, Q. Q.; Hu, X. X.; Liu, H. Y.; Zheng, W.; Chen, X. Y.; Yuan, Q.; Tan, W. H. *ACS Nano* **2017**, *11*, 8010-8017.
(46) International Fingerprint Research Group. *J. Forensic Identif.* **2014**, *64*, 174-200.
(47) Cadd, S.; Islam, M.; Manson, P.; Bleay, S. *Sci. Justice* **2015**, *55*, 219-238.

(48) Nixon, C.; Almond, M. J.; Baum J. V.; Bond, J. W. *J. Forensic Sci.* **2013**, *58*, 508-512.
(49) Peterson, R. A.; Gueniche, A.; de Beaumais, S. A.; Breton, L.; Dalko-Csiba M.; Packer, N. H. *Glycobiology* **2016**, *26*, 218-229.
(50) Fatemi, S. H. *Mol. Psychiatry*, **2005**, *10*, 251-257.
(51) Chandler K.; Goldman, R. *Mol. Cell. Proteomics*, **2013**, *12*, 836-845.
(52) Cova, M.; Oliveira-Silva, R.; Ferreira, J. A.; Ferreira, R.; Amado, F.; Daniel-da-Silva A. L.; Vitorino, R. In *Clinical Proteomics: Metods and Protocols*; Vlahou, A., Makridakis, M., Eds.; Springer Science & Business Media: New York, 2nd ed., 2015; pp 83-100.

For TOC only